

Acidification, not carbonation, is the major regulator of carbon fluxes in the coccolithophore *Emiliana huxleyi*

Dorothee M. Kottmeier, Sebastian D. Rokitta and Björn Rost

Alfred Wegener Institute, Helmholtz Centre for Polar and Marine Research, Am Handelshafen 12, 27570 Bremerhaven, Germany

Author for correspondence:

Dorothee M. Kottmeier

Tel: +49 471 48311450

Email: Dorothee.Kottmeier@awi.de

Received: 13 October 2015

Accepted: 6 January 2016

New Phytologist (2016) 211: 126–137

doi: 10.1111/nph.13885

Key words: calcification, CO₂-concentrating mechanism, life-cycle stages, membrane-inlet mass spectrometry, ocean acidification, pH, photosynthesis.

Summary

- A combined increase in seawater [CO₂] and [H⁺] was recently shown to induce a shift from photosynthetic HCO₃[−] to CO₂ uptake in *Emiliana huxleyi*. This shift occurred within minutes, whereas acclimation to ocean acidification (OA) did not affect the carbon source.
- To identify the driver of this shift, we exposed low- and high-light acclimated *E. huxleyi* to a matrix of two levels of dissolved inorganic carbon (1400, 2800 μmol kg^{−1}) and pH (8.15, 7.85) and directly measured cellular O₂, CO₂ and HCO₃[−] fluxes under these conditions.
- Exposure to increased [CO₂] had little effect on the photosynthetic fluxes, whereas increased [H⁺] led to a significant decline in HCO₃[−] uptake. Low-light acclimated cells overcompensated for the inhibition of HCO₃[−] uptake by increasing CO₂ uptake. High-light acclimated cells, relying on higher proportions of HCO₃[−] uptake, could not increase CO₂ uptake and photosynthetic O₂ evolution consequently became carbon-limited.
- These regulations indicate that OA responses in photosynthesis are caused by [H⁺] rather than by [CO₂]. The impaired HCO₃[−] uptake also provides a mechanistic explanation for lowered calcification under OA. Moreover, it explains the OA-dependent decrease in photosynthesis observed in high-light grown phytoplankton.

Introduction

Coccolithophores are unicellular calcareous algae that take a dual role in global carbon cycling. During photosynthesis, carbon dioxide (CO₂) is fixed into organic matter, leading to a net decrease in dissolved inorganic carbon (DIC) and CO₂ from seawater. In the process of calcification, calcium carbonate (CaCO₃) is precipitated, which results in lowered DIC and alkalinity, thus elevated CO₂ levels. *Emiliana huxleyi* is the most abundant coccolithophore in the present-day ocean with a distribution from tropical to subpolar waters (Winter *et al.*, 2013). The species is able to form extensive blooms (Brown & Yoder, 1994; Sadeghi *et al.*, 2012), which are often associated with a shallow mixed-layer depth and high irradiances (Nanninga & Tyrrell, 1996; Raitsos *et al.*, 2006). As one of the most important pelagic calcifiers, *E. huxleyi* has been a major focus of oceanographic research over the last decades, in particular with respect to ocean acidification (OA; e.g. Rost & Riebesell, 2004; Raven & Crawford, 2012).

As the ocean takes up anthropogenic CO₂, levels of HCO₃[−] and CO₂ increase, whereas pH and levels of CO₃^{2−} decrease (Wolf-Gladrow *et al.*, 1999). These changes in carbonate chemistry are often summarized as OA, but strictly speaking this phenomenon comprises carbonation (i.e. increased [CO₂] and [HCO₃[−]]) as well as acidification (i.e. increased [H⁺]/lowered pH). With a few exceptions, investigations of OA effects on *E. huxleyi* and other coccolithophores showed stimulated or unaffected production rates of particulate organic carbon (POC, i.e.

biomass), with concomitantly impaired or unaffected production rates of particulate inorganic carbon (PIC, i.e. CaCO₃; see Raven & Crawford, 2012, for overview). Some of the observed diversity in the OA responses could be attributed to genetic variability; but more importantly environmental factors such as irradiance were shown to modulate OA effects (Nielsen, 1997; Zondervan *et al.*, 2002; van de Poll *et al.*, 2007; Feng *et al.*, 2008; Rokitta & Rost, 2012; Sett *et al.*, 2014; Xu & Gao, 2015). OA responses are typically measured after acclimation to altered conditions over several generations, allowing cells to adjust their metabolism. A study by Barcelos e Ramos *et al.* (2010) demonstrated that the OA-induced changes in cellular POC and PIC production are already evident after a few hours, indicating that OA effects are relatively immediate. In order to identify the drivers causing the OA responses in *E. huxleyi*, Bach and co-workers disentangled the effects of carbonation and acidification by acclimating cells to artificial carbonate chemistry conditions (Bach *et al.*, 2011, 2013). In these experiments, POC and PIC production were shown to be stimulated by carbonation, but inhibited by acidification.

In order to improve our understanding of *E. huxleyi*'s response to OA, it is important to assess which cellular processes are affected by carbonation, acidification or the combination of both. *Emiliana huxleyi* is known to use CO₂ and HCO₃[−] as external inorganic carbon (C_i) sources of photosynthesis, but the estimated proportions of CO₂ uptake differ between studies and depend on the applied methods and assay conditions (e.g. Sikes

et al., 1980; Herfort *et al.*, 2002; Trimborn *et al.*, 2007; Kottmeier *et al.*, 2014). The increase in POC production after acclimation to OA is often attributed to the higher aqueous CO₂ levels, which are thought to directly increase the diffusive CO₂ supply at the CO₂-fixing enzyme Ribulose-1,5-bisphosphate-carboxylase/oxygenase (RubisCO; Raven & Johnston, 1991; Rokitta & Rost, 2012; Stojkovic *et al.*, 2013). A recent study demonstrated that the fraction of photosynthetic CO₂ uptake relative to active HCO₃⁻ uptake is indeed strongly increased under high [CO₂]/low pH (Kottmeier *et al.*, 2014). This switch in the C_i source occurred at short timescales of seconds to minutes, whereas the acclimation to OA did not significantly affect the C_i source. Thus, the beneficial OA effect seems to be directly caused by the changing carbonate chemistry rather than by changes in the expression of genes related to the CO₂-concentrating mechanism (CCM). The inhibitory effect of OA on PIC production is often attributed to changes in electrochemical gradients under high [H⁺] and the associated costs of H⁺ removal (Anning *et al.*, 1996; Berry *et al.*, 2002; Suffrian *et al.*, 2011; Taylor *et al.*, 2011). Tracer studies found HCO₃⁻ to be the major external C_i source for calcification (Paasche, 1964; Sikes *et al.*, 1980; Buitenhuis *et al.*, 1999; Herfort *et al.*, 2002; Rost *et al.*, 2002), and it was suggested that increased H⁺ levels also affect HCO₃⁻ uptake mechanisms (Fukuda *et al.*, 2014). Despite the gained knowledge on cellular processes, relatively little is known about the differential effects of carbonation and acidification on photosynthesis, calcification and their underlying C_i supply.

In order to investigate the drivers causing the immediate shifts in the photosynthetic C_i source under high [CO₂]/low pH (Kottmeier *et al.*, 2014), here we measured the photosynthetic oxygen (O₂) and C_i fluxes in direct response to carbonation, acidification and the combination of both. To this end, we acclimated both life-cycle stages of *E. huxleyi* to present-day carbonate chemistry and exposed them to a matrix of two DIC levels (1400 and 2800 μmol kg⁻¹) and two pH values (8.15 and 7.85), yielding three different CO₂ concentrations (~10, 20 and 40 μmol kg⁻¹; Fig. 1). To further address the effect of energization, cells were acclimated to low and high photon flux densities (PFD; 50 and 400 μmol photons m⁻² s⁻¹), and fluxes were measured at two different PFD (180 and 700 μmol photons m⁻² s⁻¹).

Materials and Methods

Culture conditions

The calcifying diplont (diploid life-cycle stage) *Emiliania huxleyi* (Lohmann) Hay and Mohler, strain RCC 1216, and its noncalcifying haplont, RCC 1217, were acclimated to low and high light levels (LL, 50 ± 30 μmol photons s⁻¹ m⁻²; HL, 400 ± 30 μmol photons s⁻¹ m⁻²) under present-day carbonate chemistry and a 16 h : 8 h, light : dark-cycle. Light was provided by daylight lamps (FQ 54W/965HO; OSRAM, Munich, Germany) and adjusted by measuring photon flux densities (PFD) inside water-containing culturing bottles with a Walz Universal Light meter (ULM 500; Walz, Effeltrich, Germany) using a 4π-sensor (US-SQS/L).

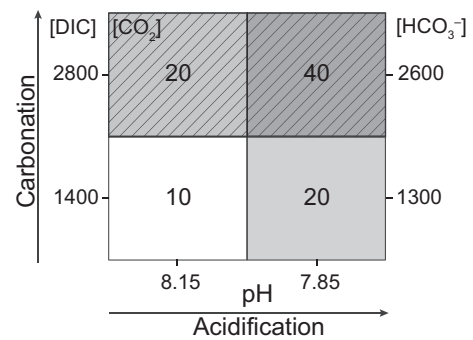


Fig. 1 Decoupled carbonate chemistry during mass spectrometric measurements of cellular O₂ and external inorganic carbon (C_i) fluxes in *Emiliania huxleyi*. Applied conditions were: low dissolved inorganic carbon (DIC)/high pH (L_{DIC}H_{pH}; white); high DIC/high pH (H_{DIC}H_{pH}; dashed, light grey); low DIC/low pH (L_{DIC}L_{pH}; light grey); high DIC/low pH (H_{DIC}L_{pH}; dashed, dark grey). All concentrations are given in μmol kg⁻¹.

Cells were grown as dilute-batch cultures in sterile-filtered North Sea seawater (0.2 μm, Sartobran 300; Sartorius AG, Göttingen, Germany) enriched with phosphate and nitrate (~7 and ~100 μmol kg⁻¹, respectively) as well as vitamins and trace metals according to F/2 (Guillard and Rytner, 1962). Culturing was performed in sterilized, gas-tight 2-l borosilicate bottles (Duran Group, Mainz, Germany), which were placed on roller tables to enable an homogenous cell suspension. Growth temperature was 15 ± 1°C and was monitored by an Almemo 28–90 data logger (Ahlborn, Holzkirchen, Germany).

In all treatments, acclimations were performed under a CO₂ partial pressure (pCO₂) of 380 μatm (38.5 Pa), representing near-present-day conditions. The pCO₂ was adjusted by pre-aerating culture media with humidified, 0.2-μm-filtered air (Midisart 2000, PTFE; Sartorius AG), containing the desired pCO₂. The gas mixture was created by a gas flow controller (CGM 2000; MCZ Umwelttechnik, Bad Nauheim, Germany) using pure CO₂ (Air Liquide, Düsseldorf, Germany) and CO₂-free air (Air purification system; Parker, Kaarst, Germany). During the acclimation, head space inside the culture bottles was minimized to avoid outgassing effects. Carbonate chemistry was monitored based on total alkalinity (TA) measurements by potentiometric titration (Dickson, 1981; TitroLine alpha plus, measurement reproducibility ± 7 μmol kg⁻¹; Schott Instruments, Mainz, Germany) and colorimetric DIC measurements with a QuAAtro autoanalyzer (measurement reproducibility ± 5 μmol kg⁻¹; Seal Analytical, Norderstedt, Germany) in sterile-filtered samples with the method of Stoll *et al.* (2001). Calculations of the carbonate system (CO₂sys; Pierrot *et al.*, 2006) were based on TA and DIC (Supporting Information Table S1). To monitor potential drifts of the carbonate chemistry on a daily basis, potentiometric measurements of pH_{NBS} were performed with a Metrohm pH meter (826 pH mobile; Metrohm, Filderstadt, Germany) with an electrode containing an integrated temperature sensor (Aquatrode Plus with Pt 1000, measurement reproducibility ± 0.01 pH units).

Cell growth was monitored by daily cell counting with a Coulter Counter (Beckman-Coulter, Fullerton, CA, USA) and specific

growth constants μ (d^{-1}) were determined as $\mu = (\log_e c_1 - \log_e c_0) \Delta t^{-1}$ (c_1 and c_0 , cell concentrations (cells ml^{-1}); Δt , time interval (d)). In both life-cycle stages, μ was more or less equal and significantly reduced in the low-light acclimations ($\sim 0.7 \text{ d}^{-1}$), confirming a light limitation in this treatment (Table S1). In the high-light treatment, μ ($\sim 1.1 \text{ d}^{-1}$) was at the upper range of previously reported growth constants for the same strain (Langer *et al.*, 2009; Rokitta & Rost, 2012).

Mass spectrometric flux measurements

Photosynthetic and respiratory O_2 and C_i fluxes were measured with a mass spectrometer (Isoprime, GV Instruments, Manchester, UK) that was coupled to a cuvette via a gas-permeable PTFE membrane (0.01 mm). This membrane-inlet mass spectrometry (MIMS) technique uses the chemical disequilibrium between CO_2 and HCO_3^- during steady-state photosynthesis to distinguish CO_2 and HCO_3^- uptake across the plasmalemma. Estimates of these fluxes were made following the equations of Badger *et al.* (1994). To include the process of calcification, we followed modifications introduced by Schulz *et al.* (2007).

The MIMS signals were calibrated for $[\text{CO}_2]$ by known additions of NaHCO_3 into phosphoric acid (0.2 N), ensuring that all added DIC was quantitatively converted to CO_2 . Baseline values were obtained by adding sodium hydroxide (0.25 mmol l^{-1}) into DIC-free media, ensuring that any residual DIC was converted CO_3^{2-} . Calibration for $[\text{O}_2]$ was obtained by equilibrating medium with air (21% O_2), followed by the addition of sufficient amounts of sodium dithionite (Merck) to quantitatively scavenge O_2 (0% O_2). MIMS signals were translated into $[\text{O}_2]$ by applying the O_2 solubility constants of seawater (Weiss, 1970). All O_2 signals were furthermore corrected for the machine-inherent consumption.

Experiments were performed with cells in their exponential growth phase with maximal cell concentrations of 5×10^4 cells ml^{-1} within 6–10 h after the start of the light period. Before the measurements, cells were concentrated to $4\text{--}10 \times 10^6$ cells ml^{-1} at acclimation temperature by gentle vacuum filtration

over polycarbonate filters (Isopore TSTP, $3 \mu\text{m}$ or RTTP, $1.2 \mu\text{m}$; Isopore membranes, Merck, Darmstadt, Germany). In this process, the medium was successively exchanged with pH-buffered DIC-free culture medium (50 mM N,N-bis(2-hydroxyethyl)-glycine, BICINE; pH_{NBS} of 7.85 or 8.15), and 8 ml were placed into an temperature-controlled MIMS cuvette in the dark. Subsequently, $25 \mu\text{mol kg}^{-1}$ membrane-impermeable dextrane-bound sulfonamide (DBS; Synthelec, Lund, Sweden) was added, inhibiting any external carbonic anhydrase. Samples were continuously stirred to keep the cell suspension homogeneously mixed. To disentangle carbonate chemistry in the cuvette, inorganic carbon was added as ~ 1400 or $\sim 2800 \mu\text{mol kg}^{-1}$ NaHCO_3 to the DIC-free medium, buffered at a pH of 8.15 or 7.85, yielding four different carbonate chemistry conditions (Fig. 1; Table 1): ‘Low DIC/High pH’ ($\text{L}_{\text{DIC}}\text{H}_{\text{pH}}$), ‘High DIC/High pH’ ($\text{H}_{\text{DIC}}\text{H}_{\text{pH}}$), ‘Low DIC/Low pH’ ($\text{L}_{\text{DIC}}\text{L}_{\text{pH}}$) and ‘High DIC/Low pH’ ($\text{H}_{\text{DIC}}\text{L}_{\text{pH}}$). For each carbonate chemistry condition, photosynthetic and respiratory O_2 and C_i fluxes were measured in consecutive light-dark intervals (6 min per step), at two different light levels (180 and $700 \mu\text{mol photons m}^{-2} \text{ s}^{-1}$).

Calculations of oxygen and carbon fluxes

Oxygen fluxes Net photosynthesis (Phot , $\mu\text{mol kg}^{-1} \text{ min}^{-1}$) and respiration (Resp , $\mu\text{mol kg}^{-1} \text{ min}^{-1}$) were deduced from steady-state O_2 fluxes in the light and dark, respectively (Badger *et al.*, 1994):

$$\text{Phot} = \frac{d\text{O}_2}{dt}_{\text{light}} \quad \text{Eqn 1}$$

$$\text{Resp} = -\frac{d\text{O}_2}{dt}_{\text{dark}} \quad \text{Eqn 2}$$

Carbonate chemistry before light (BL) For the calculation of the C_i fluxes, carbonate chemistry before and after the light phase

Acclimation	Carbonate chemistry	$\text{L}_{\text{DIC}}\text{H}_{\text{pH}}$	$\text{H}_{\text{DIC}}\text{H}_{\text{pH}}$	$\text{L}_{\text{DIC}}\text{L}_{\text{pH}}$	$\text{H}_{\text{DIC}}\text{L}_{\text{pH}}$
2N LL	$[\text{CO}_2]$	12.4 ± 0.6	22.0 ± 0.8	24.0 ± 1.5	43.7 ± 1.8
	$[\text{HCO}_3^-]$	1370 ± 70	2500 ± 90	1420 ± 80	2590 ± 110
	$[\text{H}^+]$	9.5 ± 0.2	9.5 ± 0.2	18.4 ± 0.3	18.4 ± 0.3
2N HL	$[\text{CO}_2]$	13.6 ± 0.9	22.7 ± 1.0	nd	47.4 ± 2.0
	$[\text{HCO}_3^-]$	1560 ± 110	2730 ± 130	nd	2730 ± 110
	$[\text{H}^+]$	9.1 ± 0.3	8.9 ± 0.3	nd	18.8 ± 0.3
1N LL	$[\text{CO}_2]$	10.6 ± 0.5	20.5 ± 0.3	17.1 ± 0.5	40.9 ± 2.8
	$[\text{HCO}_3^-]$	1200 ± 50	2400 ± 30	1050 ± 30	2460 ± 160
	$[\text{H}^+]$	9.2 ± 0.1	9.2 ± 0.1	17.4 ± 0.5	18.1 ± 0.0
1N HL	$[\text{CO}_2]$	10.5 ± 0.6	18.6 ± 1.4	17.9 ± 1.8	32.5 ± 2.5
	$[\text{HCO}_3^-]$	1150 ± 70	2160 ± 130	1090 ± 120	1940 ± 200
	$[\text{H}^+]$	9.3 ± 0.1	9.2 ± 0.1	17.5 ± 0.4	18.1 ± 0.5

Concentrations of CO_2 ($\mu\text{mol kg}^{-1}$), HCO_3^- ($\mu\text{mol kg}^{-1}$) and H^+ (nmol kg^{-1}) were assessed by means of mass spectrometry ($n = 3$; \pm SD).

2N LL/HL, diploid life-cycle stage acclimated to low/high light; 1N LL/HL, haploid life-cycle stage acclimated to low/high light; $\text{L}_{\text{DIC}}\text{H}_{\text{pH}}$, low dissolved inorganic carbon (DIC)/high pH; $\text{H}_{\text{DIC}}\text{H}_{\text{pH}}$, high DIC/high pH; $\text{L}_{\text{DIC}}\text{L}_{\text{pH}}$, low DIC/low pH; $\text{H}_{\text{DIC}}\text{L}_{\text{pH}}$, high DIC/low pH; nd, not determined.

Table 1 Carbonate chemistry during mass measurements of O_2 and inorganic carbon (C_i) fluxes in *Emiliana huxleyi*

was determined. $[\text{CO}_2]_{\text{BL}}$ ($\mu\text{mol kg}^{-1}$) could be directly taken from measured signals, whereas $[\text{HCO}_3^-]_{\text{BL}}$ ($\mu\text{mol kg}^{-1}$) was calculated according to Badger *et al.* (1994):

$$[\text{HCO}_3^-]_{\text{BL}} = \frac{\frac{d\text{CO}_2}{dt}_{\text{BL}} + k_+[\text{CO}_2]_{\text{BL}} - \text{Resp}/\text{RQ}}{k_-} \quad \text{Eqn 3}$$

($d\text{CO}_2/dt_{\text{BL}}$, steady-state CO_2 evolution in the dark ($\mu\text{mol kg}^{-1} \text{min}^{-1}$); k_+ and k_- , effective rate constants for the conversion of CO_2 to HCO_3^- (min^{-1}) and vice versa; RQ, respiratory quotient of 1 (Burkhardt *et al.*, 2001; Rost *et al.*, 2007)). Following Schulz *et al.* (2007), we applied the calculated effective rate constants derived from the measured pH, temperature and salinity in our assays:

$$k_- = k_{-1}[\text{H}^+] + k_{-4} \quad \text{Eqn 4}$$

$$k_+ = k_{+1} + k_{+4}[\text{OH}^-] \quad \text{Eqn 5}$$

($[\text{H}^+]$ and $[\text{OH}^-]$, concentrations of hydrogen and hydroxide ions, respectively (mol kg^{-1}); k_{-1} , k_{+1} , k_{-4} and k_{+4} , rate constants (Zeebe & Wolf-Gladrow, 2001)). To assess $[\text{H}^+]$, known $[\text{DIC}]$ ($\mu\text{mol kg}^{-1}$) was added to cell-free medium. From the resulting increase in $[\text{CO}_2]$ ($\mu\text{mol kg}^{-1}$), the ratio of $[\text{DIC}]:[\text{CO}_2]$ and thus $[\text{H}^+]$ could be derived (Zeebe & Wolf-Gladrow, 2001):

$$[\text{H}^+] = \frac{-K_1^*[\text{CO}_2] - \sqrt{(K_1^*[\text{CO}_2])^2 - 4([\text{CO}_2])^2[\text{DIC}]K_1^*K_2^*)}}{2([\text{CO}_2] - [\text{DIC}])} \quad \text{Eqn 6}$$

(K_1^* and K_2^* , stoichiometric equilibrium constants (Roy *et al.*, 1993)). $[\text{DIC}]_{\text{BL}}$ was derived as the sum of the C_i species, where carbonate ions ($[\text{CO}_3^{2-}]_{\text{BL}}$) can be assumed to be in equilibrium with $[\text{HCO}_3^-]_{\text{BL}}$ (Schulz *et al.*, 2006):

$$[\text{DIC}]_{\text{BL}} = [\text{CO}_2]_{\text{BL}} + (1 + r)[\text{HCO}_3^-]_{\text{BL}} \quad \text{Eqn 7}$$

The constant r hereby represents the pH-dependent ratio between $[\text{HCO}_3^-]$ and $[\text{CO}_3^{2-}]$ (Zeebe & Wolf-Gladrow, 2001; Schulz *et al.*, 2007), which is defined as:

$$r = \frac{[\text{CO}_3^{2-}]}{[\text{HCO}_3^-]} = \frac{K_2^*}{[\text{H}^+]} \quad \text{Eqn 8}$$

Carbonate chemistry at the end of light (EL) $[\text{CO}_2]_{\text{EL}}$ ($\mu\text{mol kg}^{-1}$) was directly obtained from measurements, whereas $[\text{HCO}_3^-]_{\text{EL}}$ ($\mu\text{mol kg}^{-1}$) was derived following Schulz *et al.* (2007):

$$[\text{HCO}_3^-]_{\text{EL}} = ([\text{DIC}]_{\text{BL}} - [\text{DIC}]_{\text{consumed}} - [\text{CO}_2]_{\text{EL}})/(1 + r) \quad \text{Eqn 9}$$

$[\text{DIC}]_{\text{consumed}}$ represents the concentration of DIC that was consumed in the course of the light interval and was defined as the

sum of DIC used for photosynthesis ($[\text{O}_2]_{\text{evolved}}/\text{PQ}$, $\mu\text{mol kg}^{-1}$) and for calcification ($[\text{DIC}]_{\text{CaCO}_3}$, $\mu\text{mol kg}^{-1}$):

$$[\text{DIC}]_{\text{consumed}} = \frac{[\text{O}_2]_{\text{evolved}}}{\text{PQ}} + [\text{DIC}]_{\text{CaCO}_3} \quad \text{Eqn 10}$$

$[\text{O}_2]_{\text{evolved}}$ hereby represents the concentration of O_2 that evolved over the course of the light phase and PQ is the photosynthetic quotient of 1.1 (Burkhardt *et al.*, 2001; Rost *et al.*, 2007). $[\text{DIC}]_{\text{CaCO}_3}$ was constrained by the measured ratio of particulate inorganic to organic carbon (PIC : POC) of the calcifying diploid life-cycle stage under similar light treatments (1.4 at low-light and 0.8 at high-light acclimations; Rokitta & Rost, 2012) and was assumed to scale linearly with $[\text{O}_2]_{\text{evolved}}$ (e.g. Paasche, 1999). Additionally, calcite production was normalized to the photoperiod (Schulz *et al.*, 2007):

$$[\text{DIC}]_{\text{CaCO}_3} = \frac{[\text{O}_2]_{\text{evolved}}}{\text{PQ}} \times \frac{16 \text{ Phot} - 8 \text{ Resp}}{16 \text{ Phot}} \times \frac{\text{PIC}}{\text{POC}} \quad \text{Eqn 11}$$

In the noncalcifying haploid stage, PIC : POC was set to zero. Sensitivity analyses in which the PIC : POC were allowed to vary within typical uncertainties, revealed negligible effects on the calculated carbonate chemistry and photosynthetic fluxes.

Carbon fluxes Knowing the carbonate chemistry, total net CO_2 uptake ($\text{CO}_2\text{up}_{\text{total}}$, $\mu\text{mol kg}^{-1} \text{min}^{-1}$) was inferred directly from the steady-state CO_2 drawdown in the light following Badger *et al.* (1994):

$$\text{CO}_2\text{up}_{\text{total}} = -\frac{d\text{CO}_2}{dt}_{\text{EL}} - k_+[\text{CO}_2]_{\text{EL}} + k_-[\text{HCO}_3^-]_{\text{EL}} \quad \text{Eqn 12}$$

Total CO_2 uptake can be divided into one part used for photosynthesis ($\text{CO}_2\text{up}_{\text{PS}}$, $\mu\text{mol kg}^{-1} \text{min}^{-1}$) and another part used for calcification ($\text{CO}_2\text{up}_{\text{CaCO}_3}$, $\mu\text{mol kg}^{-1} \text{min}^{-1}$). As HCO_3^- is the major external C_i source for calcification, we assumed that only 20% of calcification is supplied by external CO_2 (Sikes *et al.*, 1980; Paasche, 2001; Rost *et al.*, 2002). Overall calcification was constrained by photoperiod-normalized PIC : POC ratios and was assumed to scale linearly with the photosynthetic oxygen evolution:

$$\text{CO}_2\text{up}_{\text{CaCO}_3} = 0.2 \times \frac{\text{Phot}}{\text{PQ}} \times \frac{\text{PIC}}{\text{POC}} \times \frac{16 \text{ Phot} - 8 \text{ Resp}}{16 \text{ Phot}} \quad \text{Eqn 13}$$

Please note that, similar to PIC : POC ratios, errors in the assumption of the CO_2 usage for calcification can affect the estimated photosynthetic fluxes by relative constant and small offsets, but do not change the overall observed regulation patterns in response to carbonate chemistry. Accounting for the CO_2 uptake for calcification, $\text{CO}_2\text{up}_{\text{PS}}$ could be calculated as:

$$\text{CO}_2\text{up}_{\text{PS}} = \text{CO}_2\text{up}_{\text{total}} - \text{CO}_2\text{up}_{\text{CaCO}_3} \quad \text{Eqn 14}$$

Photosynthetic HCO_3^- uptake (HCO_3^- up, $\mu\text{mol kg}^{-1} \text{min}^{-1}$) was estimated as the difference between photosynthetic net C_i fixation (calculated as Phot PQ^{-1}) and net CO_2 uptake for photosynthesis:

$$\text{HCO}_3^- \text{ up} = \frac{\text{Phot}}{\text{PQ}} - \text{CO}_2\text{up}_{\text{PS}} \quad \text{Eqn 15}$$

Knowing the photosynthetic net CO_2 uptake, its fraction of the overall net photosynthetic C_i uptake (f_{CO_2} ; cf. Kottmeier *et al.*, 2014) was derived as:

$$f_{\text{CO}_2} = \text{CO}_2\text{up}_{\text{PS}} / \left(\frac{\text{Phot}}{\text{PQ}} \right) \quad \text{Eqn 16}$$

Rate normalization All rates were normalized to the amount of chlorophyll *a* (Chl*a*) in the concentrated samples. Known amounts of cell suspension were filtered onto cellulose nitrate filters (0.45 μm ; Sartorius, Gottingen, Germany) that were instantly frozen in liquid nitrogen. After extraction in 90% acetone, Chl*a* content was determined fluorimetrically (TD-700 fluorometer; Turner Designs, Sunnyvale, CA, USA) following the protocol of Knap *et al.* (1996).

Statistics

All experiments were carried out in biological triplicates. Fluxes estimated for the different carbonate chemistry conditions and at the same incoming PFD were tested pairwise for significant

differences applying two-sided *t*-tests. Effects were called significant when *P*-values were ≤ 0.05 . In the figures, such significant differences were indicated by different lower-case characters (e.g. a and b). Values denoted by two letters (e.g. ab) represent data that are not significantly different from a or b.

Results

In the following, we describe treatment-specific differences in short-term responses to altered carbonate chemistry and light. For clarity, only the fluxes of the diplont are shown in Figs 2, 3. Fluxes of the haplont are given in Table 2.

Oxygen fluxes

In both life-cycle stages and light acclimations, net photosynthesis increased under increasing incoming light (Fig. 2a,b; PFD 180 vs 700), whereas dark respiration was generally independent of the light levels applied before the dark phase (Fig. 2c,d). The dependency on carbonate chemistry was stage and acclimation-light specific (Fig. 2a–d; Table 2).

In the diplont acclimated to low light (2N LL), net photosynthesis was significantly stimulated under combined carbonation and acidification ($\text{H}_{\text{DIC}}\text{L}_{\text{pH}}$; Fig. 2a). This increase could not be attributed exclusively to carbonation or acidification, but appeared to be a product of both. Respiration in 2N LL decreased under $\text{H}_{\text{DIC}}\text{L}_{\text{pH}}$ (significantly only at PFD 180). This effect seemed to be driven by acidification, because the rates decreased significantly under both low-pH conditions, but not with carbonation (Fig. 2c).

In the diplont acclimated to high light (2N HL), net photosynthesis was significantly impaired under $\text{H}_{\text{DIC}}\text{L}_{\text{pH}}$ (Fig. 2b).

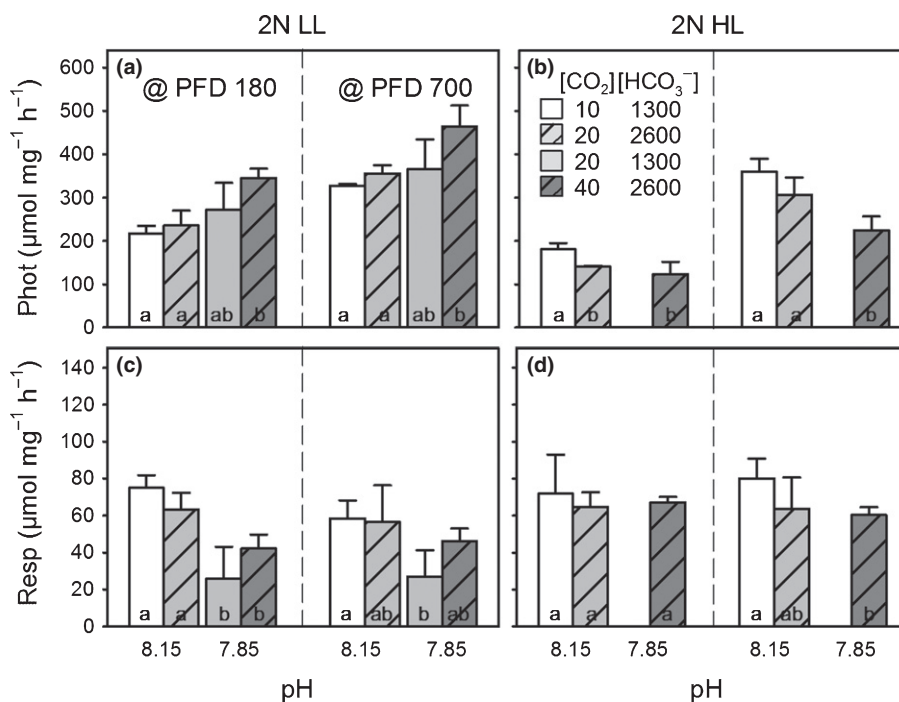


Fig. 2 Short-term modulations in photosynthetic and respiratory O_2 fluxes of *Emiliana huxleyi* in response to low dissolved inorganic carbon (DIC)/high pH ($\text{L}_{\text{DIC}}\text{H}_{\text{pH}}$; white bars), as well as carbonation ($\text{H}_{\text{DIC}}\text{H}_{\text{pH}}$; dashed, light grey bars), acidification ($\text{L}_{\text{DIC}}\text{L}_{\text{pH}}$; light grey bars) and the combination of both ($\text{H}_{\text{DIC}}\text{L}_{\text{pH}}$; dashed, dark grey bars): Chl*a*-normalized photosynthetic net O_2 evolution (Phot; a, b) and respiration (Resp; c, d) were measured at low and high photon flux densities (PFD; 180 and 700 $\mu\text{mol photons m}^{-2} \text{s}^{-1}$). Data are shown for the diploid life-cycle stage acclimated to low and high light (2N LL, 2N HL). Note: in 2N HL, no data for the $\text{L}_{\text{DIC}}\text{H}_{\text{pH}}$ condition were obtained. Error bar indicate mean \pm SD ($n = 3$). Different lower-case characters indicate significant differences between the fluxes obtained at different carbonate chemistry conditions and same PFD.

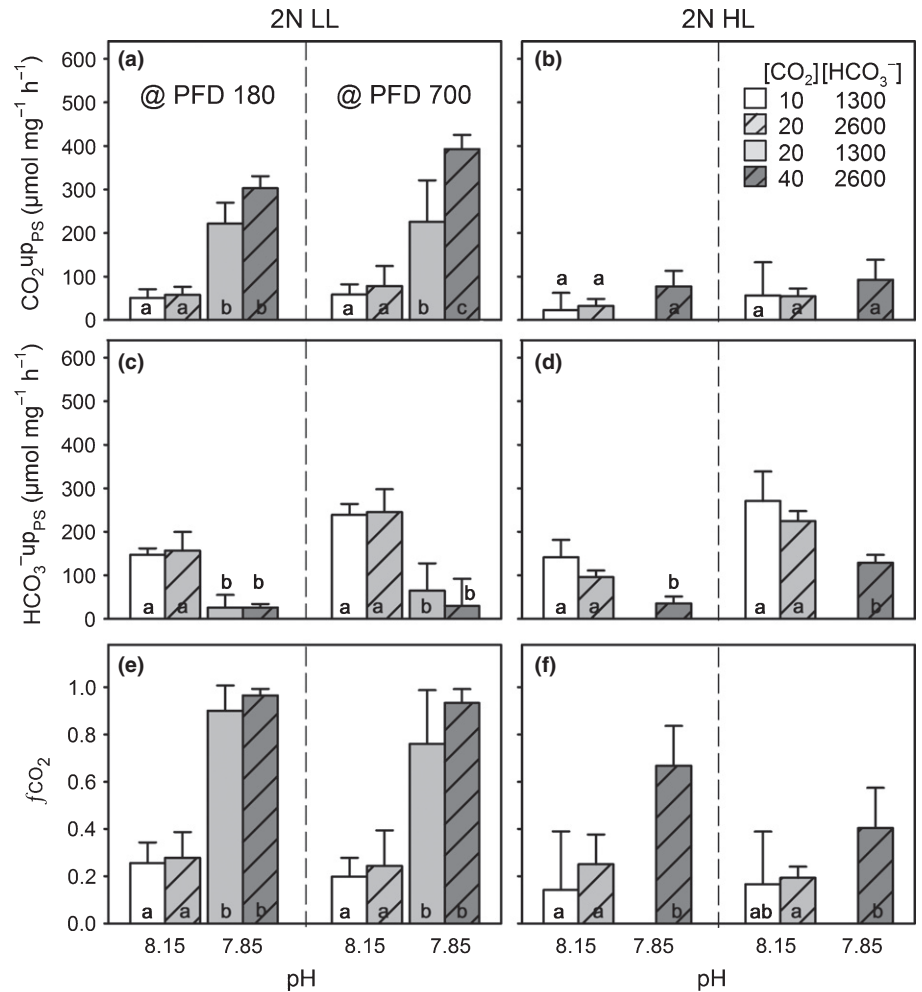


Fig. 3 Short-term modulations in external inorganic carbon (C_i) fluxes of *Emiliana huxleyi* in response to low dissolved inorganic carbon (DIC)/high pH ($L_{DIC}H_{pH}$; white bars), as well as carbonation ($H_{DIC}H_{pH}$; dashed, light grey bars), acidification ($L_{DIC}L_{pH}$; light grey bars) and the combination of both ($H_{DIC}L_{pH}$; dashed, dark grey bars): Chla-normalized photosynthetic net CO_2 uptake ($CO_2^{upt_{PS}}$; a, b), photosynthetic HCO_3^- uptake ($HCO_3^-^{upt_{PS}}$; c, d) and the fraction of overall photosynthetic net C_i uptake that is covered by net CO_2 uptake (f_{CO_2} ; e, f) were measured at low and high photon flux densities (PFD; 180 and 700 $\mu mol\ photons\ m^{-2}\ s^{-1}$). Data are shown for the diploid life-cycle stage acclimated to low and high light (2N LL, 2N HL). Note: in 2N HL, no data for the $L_{DIC}L_{pH}$ condition were obtained. Error bar indicate mean \pm SD ($n = 3$). Different lower-case characters indicate significant differences between the fluxes obtained at different carbonate chemistry conditions and same PFD.

Also this effect seemed to be caused by carbonation and acidification together, although the drivers could not be identified statistically due to the lack of the $L_{DIC}L_{pH}$ data (Fig. 1; Tables 1, 2). Respiration in 2N HL was largely unaffected by carbonate chemistry (Fig. 2d).

In contrast to the diploid, photosynthesis and respiration in the low- and high-light acclimated haplont (1N LL, 1N HL) were insensitive to the applied carbonate chemistry (Table 2).

Carbon fluxes

In both life-cycle stages and light acclimations, the higher C_i demands imposed by the higher incoming light levels during measurements were in most cases covered by additional HCO_3^- uptake, whereas photosynthetic net CO_2 uptake was largely unaffected by the incoming light (Fig. 3a–d; Table 2; PFD 180 vs PFD 700). The dependency of C_i fluxes on carbonate chemistry was clearly stage and acclimation-light specific (Fig. 3; Table 2).

In 2N LL, the photosynthetic net CO_2 uptake increased significantly under $H_{DIC}L_{pH}$ at both applied light levels, and these higher fluxes seemed to be driven mainly by acidification because CO_2 uptake was strongly increased under both low-pH conditions (Fig. 3a). Carbonation at high pH did not stimulate

the CO_2 uptake, whereas carbonation at low pH ($L_{DIC}L_{pH}$ vs $H_{DIC}L_{pH}$) additionally increased CO_2 uptake. HCO_3^- uptake in 2N LL decreased significantly under $H_{DIC}L_{pH}$ (Fig. 3c). This decrease was clearly driven by acidification because HCO_3^- uptake was decreased under both low-pH conditions, independent of carbonation. The described opposing short-term regulation of CO_2 and HCO_3^- uptake under $H_{DIC}L_{pH}$ caused significant shifts in f_{CO_2} from ~ 0.3 to ~ 0.9 (Fig. 3e).

In 2N HL, photosynthetic net CO_2 uptake was relatively unaffected by carbonate chemistry (Fig. 3b). Similar to the low-light acclimated cells, HCO_3^- uptake for photosynthesis in 2N HL decreased significantly under $H_{DIC}L_{pH}$, presumably also driven by acidification (Fig. 3d). As a consequence of the relatively constant net CO_2 uptake and the decreased HCO_3^- uptake, f_{CO_2} increased significantly from ~ 0.2 to ~ 0.7 at a PFD of 180, whereas the increase was insignificant at 700 $\mu mol\ photons\ m^{-2}\ s^{-1}$ (Fig. 3f).

In 1N LL, photosynthetic net CO_2 uptake was close to zero and the photosynthetic HCO_3^- uptake clearly dominated the C_i fluxes (Table 2). Both CO_2 and HCO_3^- fluxes were unaffected by carbonate chemistry, resulting in constant and low f_{CO_2} values (~ 0.1 on average; Table 2). In 1N HL, photosynthetic net CO_2 uptake was negative, reflecting a net CO_2 efflux alongside a high HCO_3^- uptake (Table 2). Also here, CO_2 and HCO_3^- fluxes

Table 2 Short-term modulations in photosynthetic O₂ and inorganic carbon (C_i) fluxes of *Emiliana huxleyi* in response to low dissolved inorganic carbon (DIC) and high pH (L_{DIC}H_{pH}), as well as carbonation (H_{DIC}H_{pH}), acidification (L_{DIC}L_{pH}) and the combination (H_{DIC}L_{pH})

Acclimation	PFD	Carbonate chemistry	Phot ($\mu\text{mol mg}^{-1} \text{h}^{-1}$)	Resp ($\mu\text{mol mg}^{-1} \text{h}^{-1}$)	CO ₂ upt _{PS} ($\mu\text{mol mg}^{-1} \text{h}^{-1}$)	HCO ₃ ⁻ upt _{PS} ($\mu\text{mol mg}^{-1} \text{h}^{-1}$)	f _{CO₂}
2N LL	180	L _{DIC} H _{pH}	217 ± 17	75 ± 7	51 ± 20	147 ± 15	0.26 ± 0.09
		H _{DIC} H _{pH}	236 ± 34	63 ± 9	58 ± 19	156 ± 43	0.28 ± 0.11
		L _{DIC} L _{pH}	271 ± 63	26 ± 17	221 ± 49	25 ± 29	0.90 ± 0.11
	700	H _{DIC} L _{pH}	345 ± 22	42 ± 8	303 ± 28	11 ± 9	0.96 ± 0.03
		L _{DIC} H _{pH}	327 ± 5	59 ± 10	59 ± 1	239 ± 1	0.20 ± 0.08
		H _{DIC} H _{pH}	355 ± 19	57 ± 20	78 ± 1	245 ± 1	0.24 ± 0.15
2N HL	180	L _{DIC} L _{pH}	365 ± 69	27 ± 14	226 ± 1	64 ± 1	0.76 ± 0.23
		H _{DIC} L _{pH}	464 ± 48	46 ± 7	393 ± 1	29 ± 1	0.93 ± 0.06
		L _{DIC} H _{pH}	181 ± 14	72 ± 21	23 ± 39	141 ± 40	0.14 ± 0.25
	700	H _{DIC} H _{pH}	141 ± 2	65 ± 8	32 ± 17	96 ± 15	0.25 ± 0.13
		L _{DIC} L _{pH}	nd	nd	nd	nd	nd
		H _{DIC} L _{pH}	124 ± 28	67 ± 3	77 ± 36	35 ± 16	0.67 ± 0.17
1N LL	180	L _{DIC} H _{pH}	360 ± 30	80 ± 11	56 ± 77	271 ± 68	0.17 ± 0.22
		H _{DIC} H _{pH}	307 ± 40	64 ± 17	55 ± 18	224 ± 23	0.19 ± 0.05
		L _{DIC} L _{pH}	nd	nd	nd	nd	nd
	700	H _{DIC} L _{pH}	225 ± 32	60 ± 4	93 ± 46	129 ± 18	0.40 ± 0.17
		L _{DIC} H _{pH}	147 ± 22	38 ± 8	1 ± 8	131 ± 14	0.00 ± 0.06
		H _{DIC} H _{pH}	173 ± 69	29 ± 7	28 ± 26	129 ± 39	0.15 ± 0.10
1N HL	180	L _{DIC} L _{pH}	202 ± 29	56 ± 12	58 ± 16	126 ± 19	0.31 ± 0.07
		H _{DIC} L _{pH}	185 ± 79	29 ± 3	55 ± 83	113 ± 17	0.24 ± 0.33
		L _{DIC} H _{pH}	223 ± 32	35 ± 4	-6 ± 8	207 ± 23	-0.03 ± 0.04
	700	H _{DIC} H _{pH}	240 ± 56	29 ± 5	7 ± 21	210 ± 41	0.02 ± 0.09
		L _{DIC} L _{pH}	286 ± 23	48 ± 11	26 ± 17	225 ± 25	0.11 ± 0.07
		H _{DIC} L _{pH}	273 ± 23	32 ± 4	38 ± 52	210 ± 37	0.14 ± 0.19
1N HL	180	L _{DIC} H _{pH}	119 ± 13	69 ± 4	-33 ± 7	141 ± 11	-0.31 ± 0.09
		H _{DIC} H _{pH}	113 ± 36	54 ± 8	-12 ± 26	114 ± 6	-0.18 ± 0.30
		L _{DIC} L _{pH}	136 ± 19	67 ± 19	0 ± 17	124 ± 24	0.00 ± 0.14
	700	H _{DIC} L _{pH}	148 ± 34	79 ± 20	-20 ± 17	154 ± 44	-0.14 ± 0.10
		L _{DIC} H _{pH}	246 ± 13	68 ± 8	-38 ± 10	261 ± 6	-0.17 ± 0.05
		H _{DIC} H _{pH}	196 ± 33	55 ± 9	-29 ± 24	207 ± 24	-0.18 ± 0.15
	L _{DIC} L _{pH}	236 ± 25	56 ± 8	-5 ± 8	208 ± 33	-0.02 ± 0.03	
	H _{DIC} L _{pH}	274 ± 68	75 ± 9	-23 ± 2	272 ± 60	-0.10 ± 0.03	

Chla- normalized photosynthetic net O₂ evolution (Phot) and respiration (Resp), photosynthetic net CO₂ uptake (CO₂upt_{PS}), photosynthetic HCO₃⁻ uptake (HCO₃⁻upt_{PS}) and the fraction of overall photosynthetic net C_i uptake that is covered by net CO₂ uptake (f_{CO₂}) were measured at low and high photon flux densities (PFD; 180 vs 700 $\mu\text{mol photons m}^{-2} \text{s}^{-1}$; $n = 3$; \pm SD).

2N LL/HL, diploid life-cycle stage acclimated to low light/high light; 1N LL/HL, haploid life-cycle stage acclimated to low/high light; L_{DIC}H_{pH}, low DIC/high pH; H_{DIC}H_{pH}, high DIC/high pH; L_{DIC}L_{pH}, low DIC/low pH; H_{DIC}L_{pH}, high DIC/low pH; nd, not determined.

were unaffected by carbonate chemistry, resulting in constant and negative f_{CO₂} values (~-0.1).

Discussion

In this study, we investigated *Emiliana huxleyi*'s photosynthetic O₂ and C_i fluxes and their short-term modulations in response to changing carbonate chemistry and light. In the diploid life-cycle stage (diplont), cellular fluxes were shown to be highly sensitive and to rapidly respond to the applied conditions. In the haploid stage (haplont), cellular fluxes were rather constant, even across large changes in carbonate chemistry.

H⁺-driven increase in CO₂ uptake stimulates photosynthesis in low-light acclimated diplonts

In the low-light acclimated diplont (2N LL), rates of photosynthetic O₂ evolution were in a similar range as measured earlier

under comparable conditions (Nielsen, 1995; Rokitta & Rost, 2012). They stayed relatively constant under carbonation or acidification alone, but were strongly stimulated by combined carbonation and acidification (Fig. 2a). Ocean acidification (OA) has earlier been shown to affect cellular fluxes rapidly (Barcelos e Ramos *et al.*, 2010; Kottmeier *et al.*, 2014). An immediate stimulation in photosynthesis, if maintained over longer timescales, could therefore also explain the increase in particulate organic carbon (POC) production that is typically observed in OA-acclimated coccolithophores (Raven & Crawford, 2012). Even though the applied carbonate chemistry matrix generally allowed for the distinction between the effects of carbonation and acidification, their differential effects were not evident from the observed O₂ fluxes (Fig. 2a). Only by measuring the underlying C_i acquisition was it possible to identify the drivers behind the photosynthetic responses (Fig. 3a,c): Net CO₂ uptake was strongly promoted under acidification as well as under combined carbonation and acidification (Fig. 3a), whereas HCO₃⁻ uptake

was strongly downscaled under these conditions (Fig. 3c). As the stimulation in net CO₂ uptake under combined carbonation and acidification exceeded the impairing effect on HCO₃⁻ uptake, the overall photosynthetic C_i uptake and consequently photosynthetic O₂ evolution were increased under these conditions (Fig. 2a).

The transition from the active HCO₃⁻ to diffusive CO₂ uptake under short-term acidification is in line with Kottmeier *et al.* (2014), who observed that *E. huxleyi* increases the relative fraction of CO₂ usage when being exposed to high [CO₂]/low pH over short timescales. Here we show that this shift is caused by a combination of increased CO₂ uptake and decreased HCO₃⁻ uptake. The increased CO₂ usage is likely to decrease the energy demand of the cell, because transport of HCO₃⁻ is considered more costly due to the molecule's negative charge and the large hydration envelope, properties that require an active transport (Burkhardt *et al.*, 2001; Beardall & Raven, 2004; Holtz *et al.*, 2015b). Indeed, we found stimulated photosynthesis and decreased respiration rates under acidification despite the same incoming light (Fig. 2a,c), indicating not only a more efficient CO₂ supply at RubisCO, but also altered energy allocations under these conditions. Such energy reallocations under OA have earlier been attributed to shifts from reductive towards oxidative pathways (Rokitta *et al.*, 2012).

The H⁺-driven stimulation in CO₂ uptake contradicts the 'fertilizing effect' of CO₂ that is typically ascribed to OA. Contrary to the common notion that CO₂ uptake for photosynthesis benefits from carbonation, it was here promoted mainly by acidification, at least over the short timescales applied. The higher CO₂ uptake under combined carbonation and acidification compared to acidification alone indicated that high H⁺ levels generally increase the cellular CO₂ uptake capacity. Yet, the higher CO₂ availability was able to stimulate its uptake even further – carbonation and acidification acted synergistically. The H⁺-driven decrease in cellular HCO₃⁻ uptake, which occurred independent of the applied dissolved inorganic carbon (DIC) levels, indicated that the HCO₃⁻ transport capacity is generally downscaled under acidification. Carbonation alone had no effect on HCO₃⁻ uptake, suggesting that the transporters are substrate-saturated at the applied [HCO₃⁻] (~1300 and 2600 μmol kg⁻¹). This is in line with a study by Rost *et al.* (2006) who measured the short-term DIC-dependency of photosynthesis at constant pH and showed that HCO₃⁻ uptake in *E. huxleyi* was substrate-saturated even below [HCO₃⁻] of ~500 μmol kg⁻¹.

The H⁺-dependent regulations in C_i fluxes are likely to be similar after acclimation. Bach *et al.* (2011), for instance, acclimated *E. huxleyi* to carbonate chemistry conditions in which either CO₂ or pH varied independently. They could show that POC production increases with DIC if pH is buffered to ~8.0, but it decreases with increasing DIC if pH decreases concomitantly. This suggests that the negative H⁺ effects on HCO₃⁻ uptake are retained after acclimation. However, in contrast to our study, where no short-term carbonation effects were measured, Bach and coworkers found stimulated POC and particulate inorganic carbon (PIC) production after acclimation to carbonation. Consequently, the cells were able to increase their C_i uptake when being

exposed to these conditions over longer timescales, possibly by expressing more HCO₃⁻ transporters. In order to examine how acclimation affects the sensitivity towards changing carbonate chemistry, future studies should investigate which short-term effects manifest over longer timescales.

The strong H⁺ effects on CO₂ and HCO₃⁻ uptake rates, observed in the current study, must originate from processes at the cell membrane or inside the cell, such as electrochemical gradients, enzyme activities and C_i speciation (Mackinder *et al.*, 2010; Suffrian *et al.*, 2011; Taylor *et al.*, 2011). The stimulated net CO₂ uptake under acidification could, for example, be explained by pH-dependent differences in membrane morphology (Leung *et al.*, 2012), which may also affect the CO₂ permeability. It could also be caused by pH-dependent regulations of intracellular fluxes, for instance due to different enzyme activities, which may lead to a stronger inward CO₂ gradient. The decreased HCO₃⁻ uptake under acidification is apparently caused by a direct H⁺-driven inhibition of HCO₃⁻ transporters at the plasmalemma or chloroplast membrane. The diplont *E. huxleyi* expresses AE1 and AE2-type Cl⁻/HCO₃⁻ transporters of the Solute Carrier 4 (SLC4) family (Herfort *et al.*, 2002; von Dassow *et al.*, 2009; Mackinder *et al.*, 2011; Rokitta *et al.*, 2011; Bach *et al.*, 2013). This enzyme family is well investigated in the context of renal acid/base regulation in mammals, where the activity of the anion exchangers has indeed been shown to be modulated by pH (Alper, 2006).

H⁺-driven decrease in HCO₃⁻ uptake causes carbon-limitation in high-light acclimated diplonts

In high-light acclimated diploid cells (2N HL), photosynthesis was inhibited under combined carbonation and acidification (Fig. 2b). This finding seems puzzling at first because in low-light acclimated cells (2N LL), the same carbonate chemistry had a pronounced beneficial effect on photosynthesis (Fig. 2a). However, light-dependent modulations in the sensitivity towards carbonate chemistry are well in line with other studies (e.g. Kranz *et al.*, 2010; Gao *et al.*, 2012; Rokitta & Rost, 2012; Jin *et al.*, 2013; Hoppe *et al.*, 2015). Rokitta & Rost (2012), for example, found that POC production in *E. huxleyi* is strongly stimulated when acclimated to OA and sub-saturating light, but is relatively unaffected by OA under high light intensities.

Based on our flux measurements, we are able to provide an explanation for such differential OA sensitivities: In contrast to the low-light acclimated cells, where CO₂ uptake was strongly stimulated when being exposed to acidified conditions, CO₂ uptake in the high-light acclimated cells remained unaffected (Fig. 3b). Similar to the low-light acclimated cells, HCO₃⁻ uptake in the high-light acclimated cells was impaired under acidification (Fig. 3d). As a result, the overall C_i uptake and consequently photosynthetic O₂ evolution were significantly decreased (Fig. 2b). The inability of high-light acclimated cells to increase CO₂ uptake may not only be the reason for the C_i shortage under short-term acidification, but also explains why photosynthesis is often not stimulated after acclimation to OA (Raven & Crawford, 2012). However, a detrimental H⁺ effect on

photosynthesis in *E. huxleyi* has not yet been observed after acclimation, indicating that either the decrease in HCO_3^- uptake is less pronounced, or the increase CO_2 uptake is more pronounced when cells are exposed to acidified conditions over an extended period of time.

The reduced capability of high-light acclimated cells to increase CO_2 uptake under acidification may derive from adjustments of their CO_2 -concentrating mechanism (CCM) to the higher acclimation irradiance. *Emiliana huxleyi* was shown to increase HCO_3^- uptake with increasing irradiance during flux measurements (Fig. 3d; 180 vs 700 PFD). This may indicate that high-light acclimated cells also used a higher fraction of HCO_3^- under the conditions, at which they were cultured (Rost *et al.*, 2006). Cells operating CCMs that are based predominantly on HCO_3^- uptake need to reduce the diffusive losses and therefore downregulate their CO_2 permeability, for example by altering chloroplast morphology (Sukenik *et al.*, 1987).

Recent studies on the combined effects of OA and light indicate that similar mechanisms, as here observed for *E. huxleyi*, also apply to other phytoplankton taxa. In diatoms, for example, growth was shown to increase significantly when cultured under OA and sub-saturating light, whereas these responses were reversed under high light (Gao *et al.*, 2012). Besides light intensity, light fluctuations also have been shown to significantly modulate OA effects (Jin *et al.*, 2013; Hoppe *et al.*, 2015). Hoppe and coworkers, for example, observed that photosynthesis stayed constant under OA and constant light, but decreased under OA and dynamic light. According to our data, OA may generally lower the HCO_3^- uptake capacity of phytoplankton. Although this is apparently not detrimental under low and stable light conditions, the impaired HCO_3^- uptake seems to have severe consequences under high and dynamic light conditions. Under the latter conditions, the phytoplankton cells are dependent primarily on HCO_3^- transport, because the *high* C_i demand under high light and the *varying* C_i demand under dynamic light cannot be covered or adjusted fast enough by diffusive CO_2 uptake. Owing to the impairment of HCO_3^- transporters, these cells are thus more prone to C_i shortage at RubisCO under OA, even though external substrate concentrations are slightly elevated. When RubisCO becomes C_i -limited, the Calvin Cycle is a weaker electron sink, which can cause energetic overloads and higher costs associated with dissipation of energy and repair mechanisms (van de Poll *et al.*, 2007; Gao *et al.*, 2012; Jin *et al.*, 2013; Hoppe *et al.*, 2015). Thus, the high H^+ -driven decrease in cellular HCO_3^- uptake can explain why the energy transfer efficiency from photochemistry to biomass production is reduced under OA in combination with high or dynamic light conditions (Gao *et al.*, 2012; Hoppe *et al.*, 2015).

Haplonts are insensitive to carbonate chemistry

The comparison of the two life-cycle stages of *E. huxleyi* revealed that their modes of C_i acquisition strongly diverge. Photosynthetic and respiratory O_2 fluxes in the haploid stage did not respond to the short-term changes in carbonate chemistry (Table 2). Also CO_2 and HCO_3^- uptake were not affected by

carbonation or acidification. This agrees with the results of acclimation studies that often found no or few changes in POC production and other cellular processes under OA (Rokitta & Rost, 2012; Kottmeier *et al.*, 2014). The fact that HCO_3^- uptake was unaffected by external H^+ levels implies that the HCO_3^- uptake mechanism of the haplont is different from the one of the diplont (Table 2). Indeed, there are transcriptomic datasets demonstrating that the two life-cycle stages express different isoforms of HCO_3^- transporters of the SLC4 family (von Dassow *et al.*, 2009; Mackinder *et al.*, 2011; Rokitta *et al.*, 2011). Also, the haplont was shown to express stage-specific subunits of a vacuolar H^+ ATPase and other stage-specific ion transporters, e.g. a $\text{Ca}^{2+}/\text{H}^+$ antiporters, which may further explain the differential sensitivity towards H^+ levels (von Dassow *et al.*, 2009; Rokitta *et al.*, 2011, 2012).

The consistently high HCO_3^- usage of the haplont was not in line with the results of a ^{14}C disequilibrium method, which estimated generally higher CO_2 contributions and a strong dependency on $[\text{CO}_2]/\text{pH}$ (Kottmeier *et al.*, 2014). This discrepancy may be attributed to the different key assumptions of the MIMS and/or the ^{14}C disequilibrium methods. Regarding the MIMS method, we tested the consequences of potential offsets in key assumptions (e.g. variations in rate constants, $\text{PIC}:\text{POC}$, or photosynthetic quotient (PQ)) and found that typical uncertainties cannot explain the strong deviations between the methods. In contrast to the MIMS approach, the ^{14}C disequilibrium technique does not yield actual CO_2 and HCO_3^- uptake rates, but estimates the relative CO_2 uptake for photosynthesis (Lehman, 1971; Espie & Colman, 1986; Elzenga *et al.*, 2000; Kottmeier *et al.*, 2014). In this method, f_{CO_2} is assessed based on the curvature of the cellular photosynthetic ^{14}C incorporation during a transient isotopic $^{14}\text{CO}_2$ disequilibrium in the medium. In order to estimate f_{CO_2} , the ^{14}C -incorporation is fitted with a model that is based on a number of parameters (Lehman, 1971; Espie & Colman, 1986). Some of these parameters, including kinetic constants, decay rates and the height of isotopic disequilibria remain error-afflicted and are currently being re-evaluated (S. Thoms *et al.* unpublished). Until these methodological discrepancies are better understood, the conflicting results for the haploid stage remain puzzling.

Impaired HCO_3^- uptake under acidification may affect calcification

Although the strong negative H^+ effects on photosynthetic HCO_3^- uptake have not explicitly been described before, negative H^+ effects on calcification are often discussed (Taylor *et al.*, 2011; Fukuda *et al.*, 2014; Bach *et al.*, 2015; Cyronak *et al.*, 2015). These inhibitory effects have often been attributed to changes in electrochemical gradients and the associated costs of H^+ removal (Mackinder *et al.*, 2010; Raven, 2011; Suffrian *et al.*, 2011; Taylor *et al.*, 2011). In agreement with Fukuda *et al.*, 2014, we here found strong evidence that acidification impairs the HCO_3^- uptake. Assuming that high H^+ levels affect the transport of HCO_3^- across the plasmalemma, the decreased uptake would not only influence photosynthesis, but also

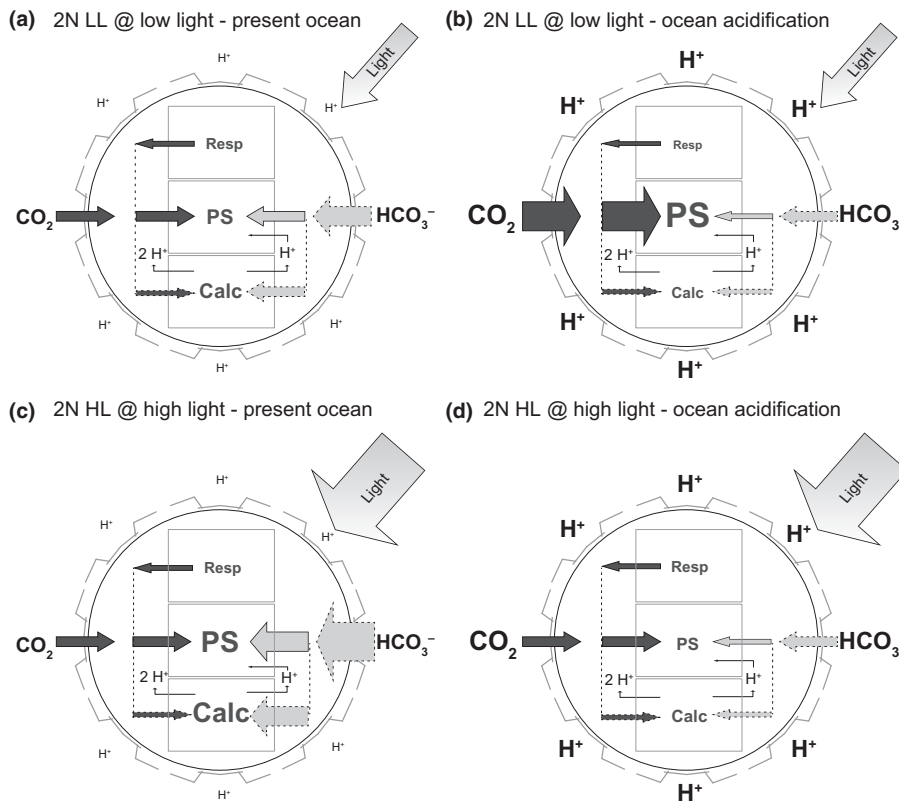


Fig. 4 Schematic illustration of the ocean acidification (OA)-dependent regulations in external inorganic carbon (C_i) fluxes of diploid, low-light acclimated (2N LL; a, b) and high-light acclimated (2N HL; c, d) *Emiliania huxleyi* under acclimation light. Sizes of arrows with solid lines reflect the measured photosynthetic and respiratory fluxes of CO_2 and HCO_3^- . Sizes of arrows with dashed lines reflect estimated fluxes. (a) Low-light acclimated cells mainly use external HCO_3^- as photosynthetic substrate under acclimation pH and achieve similar rates of calcification (Calc) and photosynthesis (PS). (b) When exposing low-light acclimated cells to OA, cells increase CO_2 uptake for photosynthesis, whereas HCO_3^- uptake is downscaled due to the increased H^+ levels. If HCO_3^- fluxes into photosynthesis and calcification were downscaled to the same degree, photosynthesis would disproportionately increase over calcification. (c) High-light acclimated cells perform higher rates of photosynthesis under acclimation light than low-light acclimated cells. The increased C_i demand is covered by additional HCO_3^- uptake. (d) When exposing high-light acclimated cells to OA, they are not able to increase CO_2 uptake rates, but nevertheless experience the H^+ -driven decrease in HCO_3^- uptake. As a consequence of the decreased overall C_i supply, photosynthesis and presumably calcification experience C_i shortage and thus decrease.

calcification. Based on flux measurements of this study, we illustrated the presumed cellular C_i fluxes in response to typical OA scenarios under different light acclimations (Fig. 4).

As HCO_3^- fluxes into POC and PIC are similar in magnitude, calcification may serve intrinsic pH regulation (Sikes *et al.*, 1980; Price *et al.*, 2008; Raven, 2011). More specifically, when HCO_3^- is used for photosynthesis, one H^+ is consumed per fixed CO_2 , and when HCO_3^- is used for calcification, one H^+ is released per produced $CaCO_3$ (Fig. 4; Holtz *et al.*, 2015a). The additional photosynthetic CO_2 uptake observed under acidification does not interfere with such a pH-homeostatic behaviour. Thus, independent of the external carbonate chemistry and light conditions, the need to exchange H^+ with the environment seems to be generally lower in the calcifying diplont of *E. huxleyi* (Fig. 4). This could provide the calcifying stage with an advantage over noncalcifying HCO_3^- users (such as the haplont), which have to assure constant H^+ uptake to compensate for alkalization during HCO_3^- -based photosynthesis (Raven, 1986, 2011). This advantage may add to the diplont's success

under bloom conditions, where seawater H^+ levels can become low.

Conclusions

In this study, we reveal a strong H^+ -driven regulation of photosynthetic C_i fluxes of *E. huxleyi* that contradicts the commonly assumed 'fertilizing effect' of CO_2 . At typical present-day conditions, HCO_3^- was shown to be the major photosynthetic C_i source of both life-cycle stages. High H^+ levels were shown to rapidly inhibit the HCO_3^- uptake and concomitantly to stimulate the CO_2 uptake. This H^+ -dependent inhibition in HCO_3^- uptake serves as a mechanistic explanation for the typical OA-dependent decline in calcification of coccolithophores and other marine calcifiers. Such an inhibition may be widespread among various phytoplankton taxa and also elucidates how the light-use efficiency can decrease when phytoplankton communities are grown under OA in combination with high or fluctuating light intensities. Future research should investigate whether similar

H⁺-dependent flux regulations are also evident when cells are acclimated to altered conditions.

Acknowledgements

We thank Klaus-Uwe Richter for the technical support and Dieter Wolf-Gladrow, Silke Thoms, Lena Holtz and Clara Hoppe for the constructive comments on this manuscript. We also gratefully acknowledge the feedback of the two anonymous reviewers. S.D.R. and B.R. received funding from the German Federal Ministry for Education and Research (BMBF) under grant no. 031A518C (ZeBiCa²) and 03F0655B (Bioacid II).

Author contributions

D.M.K., S.D.R. and B.R. planned and designed the research. D.M.K. performed experiments and analysed the data. D.M.K., S.D.R. and B.R. interpreted the data and wrote the manuscript.

References

- Alper SL. 2006. Molecular physiology of SLC4 anion exchangers. *Experimental Physiology* 91: 153–161.
- Anning T, Nimer NA, Merrett MJ, Brownlee C. 1996. Costs and benefits of calcification in coccolithophorids. *Journal of Marine Systems* 9: 45–56.
- Bach LT, Mackinder LC, Schulz KG, Wheeler G, Schroeder DC, Brownlee C, Riebesell U. 2013. Dissecting the impact of CO₂ and pH on the mechanisms of photosynthesis and calcification in the coccolithophore *Emiliania huxleyi*. *New Phytologist* 199: 121–134.
- Bach LT, Riebesell U, Gutowska MA, Federwisch L, Schulz KG. 2015. A unifying concept of coccolithophore sensitivity to changing carbonate chemistry embedded in an ecological framework. *Progress in Oceanography* 135: 125–138.
- Bach LT, Riebesell U, Schulz KG. 2011. Distinguishing between the effects of ocean acidification and ocean carbonation in the coccolithophore *Emiliania huxleyi*. *Limnology and Oceanography* 56: 2040–2050.
- Badger MR, Palmqvist K, Yu JW. 1994. Measurement of CO₂ and HCO₃[−] fluxes in cyanobacteria and microalgae during steady-state photosynthesis. *Physiologia Plantarum* 90: 529–536.
- Barcelos e Ramos J, Müller MN, Riebesell U. 2010. Short-term response of the coccolithophore *Emiliania huxleyi* to abrupt changes in seawater carbon dioxide concentrations. *Biogeosciences* 7: 177–186.
- Beardall J, Raven JA. 2004. The potential effects of global climate change on microalgal photosynthesis, growth and ecology. *Phycologia* 43: 26–40.
- Berry L, Taylor AR, Lucken U, Ryan KP, Brownlee C. 2002. Calcification and inorganic carbon acquisition in coccolithophores. *Functional Plant Biology* 29: 289–299.
- Brown CW, Yoder JA. 1994. Coccolithophorid blooms in the global ocean. *Journal of Geophysical Research-Oceans* 99: 7467–7482.
- Buitenhuis ET, De Baar HJW, Veldhuis MJW. 1999. Photosynthesis and calcification by *Emiliania huxleyi* (Prymnesiophyceae) as a function of inorganic carbon species. *Journal of Phycology* 35: 949–959.
- Burkhardt S, Amoroso G, Riebesell U, Sultemeyer D. 2001. CO₂ and HCO₃[−] uptake in marine diatoms acclimated to different CO₂ concentrations. *Limnology and Oceanography* 46: 1378–1391.
- Cyronak T, Schulz KG, Jokiel PL. 2015. The Omega myth: what really drives lower calcification rates in an acidifying ocean. *ICES Journal of Marine Science: Journal du Conseil*, fs075. doi: 10.1093/icesjms/fsv075.
- von Dassow P, Ogata H, Probert I, Wincker P, Da Silva C, Audic S, Clavierie J-M, De Vargas C. 2009. Transcriptome analysis of functional differentiation between haploid and diploid cells of *Emiliania huxleyi*, a globally significant photosynthetic calcifying cell. *Genome Biology* 10: R114.
- Dickson AG. 1981. An exact definition of total alkalinity and a procedure for the estimation of alkalinity and total inorganic carbon from titration data. *Deep-Sea Research Part II: Topical Studies in Oceanography* 28: 609–623.
- Elzenga JTM, Prins HBA, Stefels J. 2000. The role of extracellular carbonic anhydrase activity in inorganic carbon utilization of *Phaeocystis globosa* (Prymnesiophyceae): a comparison with other marine algae using the isotopic disequilibrium technique. *Limnology and Oceanography* 45: 372–380.
- Espie GS, Colman B. 1986. Inorganic carbon uptake during photosynthesis – a theoretical analysis using the isotopic disequilibrium technique. *Plant Physiology* 80: 863–869.
- Feng Y, Warner ME, Zhang Y, Sun J, Fu FX, Rose JM, Hutchins DA. 2008. Interactive effects of increased pCO₂, temperature and irradiance on the marine coccolithophore *Emiliania huxleyi* (Prymnesiophyceae). *European Journal of Phycology* 43: 87–98.
- Fukuda SY, Suzuki Y, Shiraiwa Y. 2014. Difference in physiological responses of growth, photosynthesis and calcification of the coccolithophore *Emiliania huxleyi* to acidification by acid and CO₂ enrichment. *Photosynthesis Research* 121: 299–309.
- Gao K, Xu J, Gao G, Li Y, Hutchins DA, Huang B, Wang L, Zheng Y, Jin P, Cai X *et al.* 2012. Rising CO₂ and increased light exposure synergistically reduce marine primary productivity. *Nature Climate Change* 2: 519–523.
- Guillard RRL, Ryther JH. 1962. Studies of marine planktonic diatoms. I. *Cyclotella nana* Hustedt and *Detonula confervacea* Cleve. *Canadian Journal of Microbiology* 8: 229–239.
- Herfort L, Thake B, Roberts J. 2002. Acquisition and use of bicarbonate by *Emiliania huxleyi*. *New Phytologist* 156: 427–436.
- Holtz LM, Wolf-Gladrow DA, Thoms S. 2015a. Numerical cell model investigating cellular carbon fluxes in *Emiliania huxleyi*. *Journal of Theoretical Biology* 364: 305–315.
- Holtz LM, Wolf-Gladrow DA, Thoms S. 2015b. Simulating the effects of light intensity and carbonate system composition on particulate organic and inorganic carbon production in *Emiliania huxleyi*. *Journal of Theoretical Biology* 372: 192–204.
- Hoppe CJM, Holtz L-M, Trimborn S, Rost B. 2015. Ocean acidification decreases the light use efficiency in an Antarctic diatom under dynamic but not constant light. *New Phytologist* 207: 159–171.
- Jin P, Gao K, Villafane VE, Campbell DA, Helbling EW. 2013. Ocean acidification alters the photosynthetic responses of a coccolithophorid to fluctuating ultraviolet and visible radiation. *Plant Physiology* 162: 2084–2094.
- Knap A, Michaels A, Close A, Ducklow H, Dickson A. 1996. Protocols for the joint global ocean flux study (JGOFS) core measurements. *JGOFS, Reprint of the IOC Manuals and Guides No. 29, UNESCO 1994* 19: 1–170.
- Kottmeier DM, Rokitta SD, Tortell PD, Rost B. 2014. Strong shift from HCO₃[−] to CO₂ uptake in *Emiliania huxleyi* with acidification: new approach unravels acclimation versus short-term pH effects. *Photosynthesis Research* 121: 265–275.
- Kranz SA, Levitan O, Richter KU, Prasil O, Berman-Frank I, Rost B. 2010. Combined effects of CO₂ and light on the N₂-fixing cyanobacterium *Trichodesmium* IMS101: physiological responses. *Plant Physiology* 154: 334–345.
- Langer G, Nehrke G, Probert I, Ly J, Ziveri P. 2009. Strain-specific responses of *Emiliania huxleyi* to changing seawater carbonate chemistry. *Biogeosciences* 6: 2637–2646.
- Lehman JT. 1971. Enhanced transport of inorganic carbon into algal cells and its implications for the biological fixation of carbon. *Journal of Phycology* 14: 33–44.
- Leung C-Y, Palmer LC, Qiao BF, Kewalramani S, Sknepnek R, Newcomb CJ, Greenfield MA, Vernizzi G, Stupp SI, Beyzyk MJ *et al.* 2012. Molecular crystallization controlled by pH regulates mesoscopic membrane morphology. *ACS Nano* 6: 10901–10909.
- Mackinder L, Wheeler G, Schroeder D, von Dassow P, Riebesell U, Brownlee C. 2011. Expression of biomineralization-related ion transport genes in *Emiliania huxleyi*. *Environmental Microbiology* 13: 3250–3265.
- Mackinder L, Wheeler G, Schroeder D, Riebesell U, Brownlee C. 2010. Molecular mechanisms underlying calcification in coccolithophores. *Geomicrobiology Journal* 27: 585–595.
- Nanninga HJ, Tyrrell T. 1996. Importance of light for the formation of algal blooms by *Emiliania huxleyi*. *Marine Ecology Progress Series* 136: 195–203.

- Nielsen MV. 1995. Photosynthetic characteristics of the coccolithophorid *Emiliania huxleyi* (Prymnesiophyceae) exposed to elevated concentrations of dissolved inorganic carbon. *Journal of Phycology* 31: 715–719.
- Nielsen MV. 1997. Growth, dark respiration and photosynthetic parameters of the coccolithophorid *Emiliania huxleyi* (Prymnesiophyceae) acclimated to different day length-irradiance combinations. *Journal of Phycology* 33: 818–822.
- Paasche E. 1964. A tracer study of the inorganic carbon uptake during coccolith formation and photosynthesis in the coccolithophorid *Coccolithus huxleyi*. Lund, Sweden: Scandinavian Society for Plant Physiology.
- Paasche E. 1999. Reduced coccolith calcite production under light-limited growth: a comparative study of three clones of *Emiliania huxleyi* (Prymnesiophyceae). *Phycologia* 38: 508–516.
- Paasche E. 2001. A review of the coccolithophorid *Emiliania huxleyi* (Prymnesiophyceae), with particular reference to growth, coccolith formation, and calcification–photosynthesis interactions. *Phycologia* 40: 503–529.
- Pierrot D, Lewis E, Wallace D. 2006. *MS Excel program developed for CO₂ system calculations*. ORNL/CDIAC-105. Oak Ridge, TN, USA: Carbon Dioxide Information Analysis Center, Oak Ridge National Laboratory, US Department of Energy.
- van de Poll WH, Visser RJ, Buma AG. 2007. Acclimation to a dynamic irradiance regime changes excessive irradiance sensitivity of *Emiliania huxleyi* and *Thalassiosira weissflogii*. *Limnology and Oceanography* 52: 1430–1438.
- Price GD, Badger MR, Woodger FJ, Long BM. 2008. Advances in understanding the cyanobacterial CO₂-concentrating-mechanism (CCM): functional components, C_i transporters, diversity, genetic regulation and prospects for engineering into plants. *Journal of Experimental Botany* 59: 1441–1461.
- Raitsos D, Lavender S, Pradhan Y, Tyrrell T, Reid P, Edwards M. 2006. Coccolithophore bloom size variation in response to the regional environment of the subarctic North Atlantic. *Limnology and Oceanography* 51: 2122–2130.
- Raven J. 1986. Biochemical disposal of excess H⁺ in growing plants? *New Phytologist* 104: 175–206.
- Raven J. 2011. Effects on marine algae of changed seawater chemistry with increasing atmospheric CO₂. *Biology and Environment: Proceedings of the Royal Irish Academy* 111 B: 1–17.
- Raven J, Crawford K. 2012. Environmental controls on coccolithophore calcification. *Marine Ecology Progress Series* 470: 137–166.
- Raven J, Johnston A. 1991. Mechanisms of inorganic carbon acquisition in marine phytoplankton and their implications for the use of other resources. *Limnology and Oceanography* 36: 1701–1714.
- Rokitta S, De Nooijer L, Trimborn S, De Vargas C, Rost B, John U. 2011. Transcriptome analyses reveal differential gene expression patterns between life-cycle stages of *Emiliania huxleyi* (Haptophyta) and reflect specialization to different ecological niches. *Journal of Phycology* 47: 829–838.
- Rokitta S, John U, Rost B. 2012. Ocean acidification affects redox-balance and ion-homeostasis in the life-cycle stages of *Emiliania huxleyi*. *PLoS ONE* 7: e52212.
- Rokitta S, Rost B. 2012. Effects of CO₂ and their modulation by light in the life-cycle stages of the coccolithophore *Emiliania huxleyi*. *Limnology and Oceanography* 57: 607–618.
- Rost B, Kranz SA, Richter KU, Tortell PD. 2007. Isotope disequilibrium and mass spectrometric studies of inorganic carbon acquisition by phytoplankton. *Limnology and Oceanography – Methods* 5: 328–337.
- Rost B, Riebesell U. 2004. Coccolithophores and the biological pump: responses to environmental changes. In: Thierstein HR, Young JR, eds. *Coccolithophores – from molecular processes to global impact*. Heidelberg, Germany: Springer, 76–99.
- Rost B, Riebesell U, Sültemeyer D. 2006. Carbon acquisition of marine phytoplankton: effect of photoperiod length. *Limnology and Oceanography* 51: 12–20.
- Rost B, Zondervan I, Riebesell U. 2002. Light-dependent carbon isotope fractionation in the coccolithophorid *Emiliania huxleyi*. *Limnology and Oceanography* 47: 120–128.
- Roy RN, Roy LN, Vogel KM, Porter Moore C, Pearson T, Good CE, Millero J, Campbell DM. 1993. The dissociation constants of carbonic acid in seawater at salinities 5 to 45 and temperatures 0 to 45°C. *Marine Chemistry* 44: 249–267.
- Sadeghi A, Dinter T, Vountas M, Taylor B, Altenburg-Soppa M, Bracher A. 2012. Remote sensing of coccolithophore blooms in selected oceanic regions using the PhytoDOAS method applied to hyper-spectral satellite data. *Biogeosciences* 9: 2127–2143.
- Schulz KG, Riebesell U, Rost B, Thoms S, Zeebe RE. 2006. Determination of the rate constants for the carbon dioxide to bicarbonate inter-conversion in pH-buffered seawater systems. *Marine Chemistry* 100: 53–65.
- Schulz KG, Rost B, Burkhardt S, Riebesell U, Thoms S, Wolf-Gladrow DA. 2007. The effect of iron availability on the regulation of inorganic carbon acquisition in the coccolithophore *Emiliania huxleyi* and the significance of cellular compartmentation for stable carbon isotope fractionation. *Geochimica et Cosmochimica Acta* 71: 5301–5312.
- Sett S, Bach LT, Schulz KG, Koch-Klavsen S, Lebrato M, Riebesell U. 2014. Temperature modulates coccolithophorid sensitivity of growth, photosynthesis and calcification to increasing seawater pCO₂. *PLoS ONE* 9: e88308.
- Sikes CS, Roer RD, Wilbur KM. 1980. Photosynthesis and coccolith formation: inorganic carbon sources and net inorganic reaction of deposition. *Limnology and Oceanography* 25: 248–261.
- Stojkovic S, Beardall J, Matear R. 2013. CO₂-concentrating mechanisms in three southern hemisphere strains of *Emiliania huxleyi*. *Journal of Phycology* 49: 670–679.
- Stoll MHC, Bakker K, Nobbe GH, Haese RR. 2001. Continuous-flow analysis of dissolved inorganic carbon content in seawater. *Analytical Chemistry* 73: 4111–4116.
- Suffrian K, Schulz KG, Gutowska MA, Riebesell U, Bleich M. 2011. Cellular pH measurements in *Emiliania huxleyi* reveal pronounced membrane proton permeability. *New Phytologist* 190: 595–608.
- Sukenik A, Bennett J, Falkowski P. 1987. Light-saturated photosynthesis – limitation by electron transport or carbon fixation. *Biochimica et Biophysica Acta* 891: 205–215.
- Taylor AR, Chrachri A, Wheeler G, Goddard H, Brownlee C. 2011. A voltage-gated H⁺ channel underlying pH homeostasis in calcifying coccolithophores. *PLOS Biology* 9: e1001085.
- Trimborn S, Langer G, Rost B. 2007. Effect of varying calcium concentrations and light intensities on calcification and photosynthesis in *Emiliania huxleyi*. *Limnology and Oceanography* 52: 2285–2293.
- Weiss RF. 1970. The solubility of nitrogen, oxygen and argon in water and seawater. *Deep-Sea Research* 17: 721–735.
- Winter A, Henderiks J, Beaufort L, Rickaby REM, Brown CW. 2013. Poleward expansion of the coccolithophore *Emiliania huxleyi*. *Journal of Plankton Research* 36: 316–325.
- Wolf-Gladrow DA, Riebesell U, Burkhardt S, Bijma J. 1999. Direct effects of CO₂ concentration on growth and isotopic composition of marine plankton. *Tellus Series B – Chemical and Physical Meteorology* 51: 461–476.
- Xu K, Gao K. 2015. Solar UV Irradiances modulate effects of ocean acidification on the coccolithophorid *Emiliania huxleyi*. *Photochemistry and Photobiology* 91: 92–101.
- Zeebe RE, Wolf-Gladrow DA. 2001. *CO₂ in seawater: equilibrium, kinetics, isotopes*. Amsterdam, the Netherlands: Elsevier Science B.V.
- Zondervan I, Rost B, Riebesell U. 2002. Effect of CO₂ concentration on the PIC/POC ratio in the coccolithophore *Emiliania huxleyi* grown under light-limiting conditions and different daylengths. *Journal of Experimental Marine Biology and Ecology* 272: 55–70.

Supporting Information

Additional supporting information may be found in the online version of this article.

Table S1 Acclimation carbonate chemistry

Please note: Wiley Blackwell are not responsible for the content or functionality of any supporting information supplied by the authors. Any queries (other than missing material) should be directed to the *New Phytologist* Central Office.